Available online at www.CivileJournal.org

Civil Engineering Journal

(E-ISSN: 2476-3055; ISSN: 2676-6957)

Vol. 11, No. 04, April, 2025

Strength, Water Porosity and Sulfuric Acid Performance of Coconut Fiber Reinforced High-Strength Concrete

Gervany Hurlich Mboungou Londe [1*], John Nyiro Mwero [2], Christopher Kanali [3], Sylvester Ochieng Abuodha [4]

[1] *Department of Civil Engineering, Institute for Basic Sciences Technology and Innovation Hosted at Jomo Kenyatta University of Agriculture and Technology (JKUAT), Pan-African University, Nairobi, Kenya.*

[2] *Department of Civil and Construction Engineering, Technical University of Kenya (TUK), Nairobi, Kenya.*

[3] *Department of Agricultural and Biosystems Engineering, Jomo Kenyatta University of Agriculture and Technology (JKUAT), Nairobi, Kenya.*

[4] *Department of Civil and Construction Engineering, University of Nairobi (UoN), Nairobi, Kenya.*

Received 11 November 2024; Revised 11 March 2025; Accepted 18 March 2025; Published 01 April 2025

Abstract

This study investigates the use of coconut fibers (CFs) derived from coconut husks to enhance the performance of high-strength concrete (HSC), aligning with sustainability goals through the reuse of agricultural waste. The objective was to assess the strength properties, water porosity, and sulfuric acid resistance of coconut fiber-reinforced high-strength concrete (CFR-HSC), targeting a mean compressive strength of 60 MPa. CFs underwent an alkali treatment involving boiling for one hour followed by immersion in a 1% sodium hydroxide (NaOH) solution, which improved their surface morphology as confirmed by scanning electron microscopy (SEM). Concrete specimens with CFs contents of 0.25, 0.5, 1.0, 1.5, and 2.0% were evaluated. Increased CF contents content reduced workability and dry density, while compressive strength at 7 and 14 days improved by 2.31 and 13.02%, respectively, at 0.5% CF content but showed no significant improvement at 28 days. However, tensile and flexural strengths improved significantly, achieving the highest gains of 34.71 and 7.03% at 1% CF content, respectively. CFR-HSC exhibited increased water porosity but enhanced resistance to sulfuric acid, indicating improved durability under aggressive environments. These findings demonstrate the potential of NaOH-treated (NT) CFs to enhance tensile and flexural properties while improving chemical durability, offering a sustainable approach to advancing HSC performance.

Keywords: Coconut Fiber Reinforced High-Strength Concrete; Workability; Strength; Water Porosity; Sulfuric Acid.

1. Introduction

Concrete is the most widely used construction material globally, valued for its versatility and high compressive strength. Its ability to be molded into various shapes and sizes makes it ideal for diverse applications, including buildings, bridges, roads, dams, and tunnels. However, traditional concrete faces challenges due to its limited tensile strength, low ductility, and the growing environmental concerns associated with its production [1, 2]. Sustainable development seeks to balance human needs with environmental preservation, ensuring the conservation of natural resources for future generations. In construction, this goal translates into developing materials that are not only strong and durable but also eco-friendly [3, 4]. One promising avenue for sustainable construction is the incorporation of plant-based fibers into concrete. This approach provides a greener, more resource-efficient alternative while maintaining the mechanical

* Corresponding author: gervanymboungou@gmail.com; londe.mboungou@students.jkuat.ac.ke

http://dx.doi.org/10.28991/CEJ-2025-011-04-023

strength and durability of cement composites [5, 6]. The rising interest in plant-based fibers stems from their sustainable properties compared to synthetic fibers. Plant-based fibers like coconut, sisal, hemp, jute, kenaf, etc. are abundant, affordable, renewable, and biodegradable, making them a more environmentally friendly option [7, 8]. Studies have demonstrated that these fibers can enhance the mechanical properties of concrete, such as improving tensile strength, toughness, and crack resistance [9, 10]. Furthermore, their lightweight nature and compatibility with cement matrices contribute to enhanced durability and reduced overall material density [11]. The growing use of plant-based fibers aligns with the increasing demand for sustainable construction practices, helping to mitigate the environmental impacts of synthetic fiber production and disposal. This shift underscores the importance of adopting innovative materials and techniques to support a more sustainable and environmentally conscious construction industry. Research on natural and recycled fibers, including coconut fibers (CFs), highlights their potential in creating sustainable, greener concrete [12, 13].

The incorporation of small, evenly distributed, and randomly oriented plant-based fibers effectively minimizes drying shrinkage by limiting microcracks and strengthening the concrete matrix [14]. Due to their high tensile strength and elasticity, these fibers enhance the mechanical properties of concrete by efficiently transferring stress during loading [15]. They contribute to improved tensile and flexural strength, better crack control, increased impact resistance, enhanced fracture toughness, and modifications to the concrete's rheological behavior [5, 16, 17].

Concrete reinforced with plant-based fibers can surpass traditional materials in mechanical performance, as these fibers delay crack initiation and effectively control crack propagation. By restricting the growth of microcracks, they reduce the likelihood of sudden failure [6]. The resulting hardened matrix exhibits shorter cracks, which significantly improves the composite's impermeability and durability under environmental exposure [18]. Additionally, fiber-reinforced concrete maintains its load-bearing capacity even after cracking, with notable improvements in tensile and flexural strength due to the fibers enhancing residual strength.

The effectiveness of fiber reinforcement is influenced by various factors, including the matrix characteristics, fiber type and content, fiber size and volumetric fraction, the concrete-fiber application process, and the shape of the element being reinforced [19]. However, a high volumetric fraction of fibers can negatively impact compressive strength and workability, often resulting in reduced concrete strength due to poor fiber-matrix bonding [20, 21]. Moreover, the orientation of fibers relative to the cracks significantly affects their efficiency in enhancing mechanical properties [22, 23]. The fibers' contribution to performance is most effective when they are aligned perpendicular to crack openings in the direction of stress [24, 25].

Porosity is a critical property to consider when designing concrete mixtures, as it directly influences both the durability and the mechanical performance of concrete [26]. High porosity facilitates the ingress of aggressive agents, leading to reinforcement corrosion and microstructural damage [27, 28]. This accelerates deterioration, particularly under cyclic environmental conditions and extreme climates [29]. Moreover, increased porosity weakens the cementitious matrix and interfacial transition zones, significantly reducing compressive strength [30, 31]. Numerous studies highlight the impact of porosity on concrete's mechanical properties and durability, along with the variety of testing methods available [32, 33]. CF reinforced concrete adds complexity to porosity due to the high-water absorption of CFs, which increases the water/cement ratio and slows water evaporation, resulting in higher porosity [34]. The finer fractions of these fibers further aggravate porosity in interfacial transition zones [35].

This research evaluated three types of porosity in concrete: total, capillary, and air, using water porosity tests based on traditional methods that measure water absorption through total immersion or capillary action, focusing on pores accessible to water [36, 37]. Total porosity represents the proportion of voids in concrete that can retain water, with higher levels often linked to reduced durability due to water ingress, which can cause degradation, chemical attacks, and reinforcement corrosion [38]. Capillary porosity, or open porosity, consists of interconnected voids that allow the passage of fluids and gases, increasing the concrete's sensitivity to environmental factors and accelerating its degradation when excessive. Meanwhile, air porosity, or closed porosity, is composed of isolated voids that prevent fluid movement but may compromise compressive strength and raise permeability.

Despite the significant advantages offered by plant-based fibers, their organic composition makes them prone to degradation in concrete, due to environmental factors and the chemically aggressive nature of the cementitious matrix [39]. Research has shown that this degradation is primarily driven by the highly alkaline environment created during cement hydration, where the formation of $Ca(OH)_2$ plays a key role [40–43]. Exposure of plant-based fibers to the alkaline pore solution accelerates degradation, increasing porosity, internal strain, moisture absorption, chemical breakdown, and reducing mechanical properties [44]. Moreover, the bond between the fibers and the cement matrix is often weak due to the hydrophilic nature of plant-based fibers [45]. The hydroxyl groups present in these fibers attract water molecules, exacerbating the issue. To address these challenges, various treatment methods, including chemical and thermal techniques, have been developed [46]. These treatments aim to enhance the fiber-matrix bond and reduce moisture movement in and around the fibers during wetting and drying cycles [47]. Additionally, the use of silica fume has been shown to create a localized pozzolanic reaction, which protects plant-based fibers and improves their resistance to chlorides [39].

Plant-based fibers, including CFs, have been shown to enhance the tensile and flexural properties of concrete [48]. However, studies often neglect the combined effects of mechanical properties, water porosity, and chemical durability under aggressive environments, especially in high-strength concrete (HSC). These fibers can disrupt the cementitious matrix and increase porosity by creating additional interfacial zones [49]. Adjusting water content to maintain workability when incorporating fibers further contributes to porosity [50]. The interaction between fiber type and concrete components significantly influences water demand and workability [51–53]. Challenges such as fiber degradation in alkaline environments and weak bonding with the cement matrix persist. Although various fiber treatment methods have been explored, their effects on HSC performance under combined mechanical and chemical conditions remain insufficiently studied. Additionally, research on the impact of varying fiber content to optimize workability, strength, and durability is still limited.

This study addresses these gaps by investigating the use of NaOH-treated CFs (boiling followed by sodium hydroxide treatment) as reinforcement in HSC to assess their impact on compressive, tensile, and flexural strengths, water porosity, and sulfuric acid resistance. By varying fiber content and focusing on sustainability through agricultural waste reuse, the research aims to optimize the fiber-matrix interaction and enhance the durability of HSC under aggressive environments. Additionally, the study seeks to provide new insights into the trade-offs between fiber content, workability, dry density and overall performance.

2. Materials and Methods

2.1. Material Locations and Properties

In this study, Portland-pozzolanic cement (CEM II/B-P 42.5 N) was used, which was locally manufactured in Nairobi, Kenya, and met the EN 197 standard [54]. The chemical properties of this cement are detailed in Table 1. The coarse aggregate (CA) was crushed stone with a maximum size of 12.50 mm, sourced from Mlolongo quarries in Nairobi, Kenya. The fine aggregate (FA) was river sand with a maximum size of 5 mm, also obtained from Mlolongo quarries. To improve the workability of the concrete, Sika Viscoflow 615 KE superplasticizer (SP), produced by Sika Chemicals in Nairobi, Kenya, was used. Sodium hydroxide (NaOH) pellets with a purity of 97% were acquired in Nairobi, Kenya. Potable water from the JKUAT water pump was used for all concrete mixes. The CFs were extracted from mature husks in Mombassa, Kenya, a well-known area for coconut abundance. A summary of the materials used in this research is provided in Table 2.

Table 1. Chemical properties of CEM II/B-P 42.5 N

Chemical Analysis				
Parameter	**Abbreviation**	**Specification**	**Unit**	**Result**
Loss on Ignition	LOI	-	%	4.19
Silicon Dioxide	SiO_2	-		24.42
Insoluble Residue	I.R.	-		12.05
Aluminium Oxide	Al_2O_3	-		6.02
Iron Oxide	Fe_2O_3	-		3.75
Calcium Oxide	CaO	-		57.06
Magnesium Oxide	MgO	-		1.28
Sulfur Trioxide	SO_3	≤3.5		2.66
Sodium Oxide	Na_2O	-		0.84
Potassium Oxide	K_2O	-		8.92
Pozzolanicity	-	-		Pass
Chloride	Cl-	≤0.1		<0.01

Table 2. Summary of materials to be used for concrete production

Materials	Properties
Fine aggregate (River sand)	Maximum size of 5 mm
Coarse aggregate (Crushed stone)	Maximum size of 12.50 mm
Sodium Hydroxide (NaOH)	97% Extra pure
CEM II/B-P 42.5 N	Specific gravity of 2.86
Superplasticizer (SP)	Specific gravity of 1.08
Water	Specific gravity of 1.00
Untreated coconut fiber	Specific gravity of 1.18
Boil-treated coconut fiber	Specific gravity of 1.16
boiled, and then treated with NaOH	Specific gravity of 1.25

2.2. Characterization of Aggregates

The suitability of FA and CA for concrete was evaluated by examining their particle size distribution (Figure 1). Prior to usage, both FA and CA were thoroughly cleaned to remove impurities and sun-dried to remove moisture. The aggregates were then sieved and graded according to ASTM C33 standards [55], adhering to the defined upper and lower limits. The findings indicated that both aggregates were suitable for concrete mixtures as per ASTM C136 [56]. CA sizes varied from 12.5 to 2.36 mm (Figure 2(a)), meaning they passed through a 12.5 mm sieve and were retained by a 2.36 mm sieve. The maximum size for FA was 5 mm, as shown in Figure 2(b). The fineness modulus of FA and CA was 2.50 and 2.41, respectively, conforming to the ASTM C136 requirement for concrete aggregates, which specifies a fineness modulus range of 2.3 to 3.1.

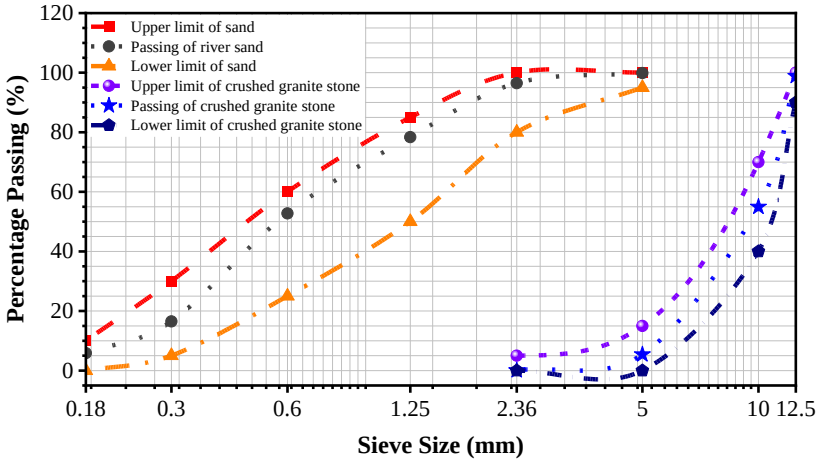

Figure 1. Size distribution of fine and coarse aggregates

Figure 2. Images of aggregates used in concrete

2.3. Physical and Mechanical Properties of Aggregates

The characteristics of the FA and CA utilized in this study are summarized in Table 3. The rodded dry bulk density for FA and CA intended for the mixture was measured at 1680 and 1515 kg/m³, respectively, meeting the BS 812-2 [57] standard for bulk density-dry rodded aggregates in concrete, falling within the range of 1400 to 1800 kg/m³. The specific gravity on an oven-dry basis for FA and CA was recorded as 2.54 and 2.47, respectively, in accordance with ASTM C127 [58] specifications. For CA, the aggregate impact value (AIV) was 4.07% and the aggregate crush value (ACV) was 14.76%, both below the permissible limits of 10 and 30%, as stipulated by BS 812-112 [59] and BS 812-110 [60]. These results affirm that the aggregates are suitable for use in concrete applications.

Table 3. Physical and mechanical properties of fine and coarse aggregates

Properties	Fine aggregate	Coarse aggregate
Specific gravity on an oven-dry basis	2.54	2.47
Apparent specific gravity on an oven-dry basis	2.73	2.72
Water absorption (%)	2.81	3.7
Bulk density-dry rodded (kg/m^3)	1680	1515
Fineness modulus	2.5	2.41
Aggregate impact value (%)	-	4.07
Aggregate crush value (%)	-	14.76

2.4. Extraction and Treatment of Coconut Fibers

The coconut husks were soaked in water for three days to make fiber extraction easier and to remove contaminants and soil. The fibers were then cleaned with potable water and sun-dried before further processing. Next, the fibers were boiled by placing them in a pot of water at boiling point, as shown in Figure 3(c). This crucial step prepares fibers for subsequent processing. To achieve the boiling treatment (BT), the fibers underwent vigorous bubbling and heating for an hour, leading to significant changes. The heat and agitation helped break down certain components, separate impurities, and enhance the cleanliness of the fibers. Boiling also softened the fibers, making them more flexible for further processing. After boiling, the fibers were soaked in a 1% NaOH solution for 60 minutes to obtain the Alkali or NaOH treatment (NT), as shown in Figure 3 and 4. The fibers were then thoroughly washed with potable water until the pH reached a neutral level (pH 7 ± 0.5). This washing process removed any residual alkali. Finally, the CFs were disintegrated and sun-dried. This treatment changed the surface properties of the fibers, improving their chemical reactivity and ability to bond with cement paste. This study assessed the mechanical properties and durability of HSC reinforced with NT CFs. The CFs were cut into length of 20 ± 2mm to be used in concrete.

Figure 3. Processing of coconut fibers: (a) collection of coconut fibers, (b) washing of coconut fibers, (c) boiling of coconut fibers, (d) NaOH container, and (e) drying of coconut fibers

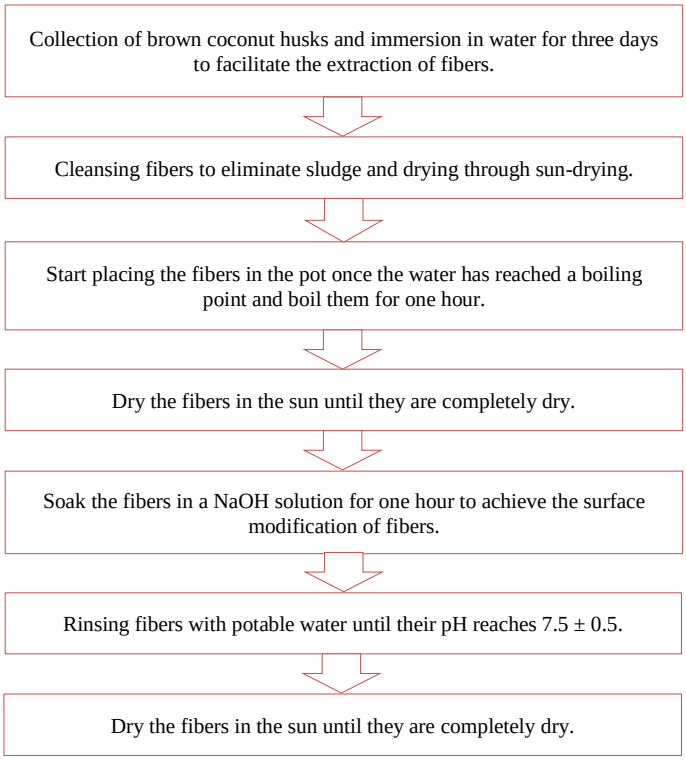

Figure 4. Flowchart for treatment of coconut fibers

2.5. Scanning Electron Microscopy (SEM) of Coconut Fibers

The morphological properties of untreated (UT), BT and NT CFs were analyzed using scanning electron microscopy (SEM). Random fiber samples from each group were affixed to aluminum SEM stubs with carbon adhesive tape and then coated with carbon to improve conductivity. Imaging was done using a TESCAN MIRA SEM, while elemental analysis was carried out with a Thermo Fisher Nova NanoSEM equipped with an Oxford X-Max detector and INCA software.

2.6. Concrete Mix Design

The target mean compressive strength was set at 60 MPa using a concrete mix designed according to ACI 211.4R [61], with a water-cement ratio (W/C) of 0.35. To address the high-water absorption of CFs, a SP was added at 2% by weight of cement in each mix to improve workability. Concrete with various CF contents, ranging from 0.25 to 2% by weight of cement, were tested. Additional details on the mixes are provided in Table 4.

Table 4. Concrete mix proportions

Mix	CF (%)	kg/m^3						W/C ratio
		Cement	CF	Water	SP	FA	CA	
Mix 1	0	500	0	175	10	679	1060	0.35
Mix 2	0.25	500	1.25	175	10	679	1060	0.35
Mix 3	0.50	500	2.50	175	10	679	1060	0.35
Mix 4	1	500	5	175	10	679	1060	0.35
Mix 5	1.50	500	7.50	175	10	679	1060	0.35
Mix 6	2	500	10	175	10	679	1060	0.35

2.7. Procedure of Casting and Curing Concrete

A rotary drum mixer was used to combine all the components: coarse aggregate (CA), fine aggregate (FA), cement, water, superplasticizer (SP), and CFs. The CA was categorized into three size ranges: 2.36–5 mm (5% by weight of CA), 5–10 mm (25% by weight of CA), and 10–12.5 mm (70% by weight of CA). Water and SP were premixed to form a lubricant, which was gradually added to the mixer along with CFs to ensure uniform distribution. The workability of the fresh concrete was assessed using a slump test, as illustrated in Figure 5. The concrete was then poured into oiled molds and compacted using an electric vibrator.

After 24 hours, the samples were demolded and water-cured to ensure proper hydration, prevent premature drying, and minimize shrinkage. The curing durations were 7, 14, and 28 days for mechanical testing, 56 days for water porosity tests, and 28 and 56 days for sulfuric acid resistance tests. Different molds were used based on the type of test, as shown in Figure 6. Cubical samples were used for compressive strength, dry density, water porosity, and sulfuric acid resistance tests. In addition, cylindrical samples were used for split tensile strength tests, while prismatic samples were used for flexural strength tests.

Figure 5. Slump test: (a) control concrete, (b) concrete with a low fiber content, and (c) concrete with a high fiber content

Figure 6. Concrete cast into cube, cylinder, and beam specimens

3. Experimental Procedures and Testing Method

3.1. Mechanical Strength Tests of Concrete

Compressive Strength Test

Compressive strength (f_c), was assessed using 100 × 100 × 100 mm concrete cubes. The samples were cured in water for 7, 14 and 28 days before being tested. The tests were carried out using a universal testing machine, Figure 7 (a) with a capacity of 1500 kN, applying a load of 0.5 kN/s in accordance with EN 12390-3 [62]. For each curing period, the average compressive strength was calculated from the results of three samples. The compressive strength was determined by dividing the maximum load supported (P_{max}) by the specimen by its cross-sectional area (A), as expressed in Equation 1:

$$f_c = \frac{P_{max}}{A} \quad (1)$$

(a) (b) (c)

Figure 7. Mechanical test setup: (a) compressive test, (b) split tensile test, and (c) flexural test

Split Tensile Strength Test

Splitting tensile strength (f_{st}), was determined using cylindrical specimens with dimensions of 100 mm in diameter (D) and 200 mm in length (L). The specimens were subjected to water curing for 7, 14, or 28 days before testing. Testing was performed on a universal testing machine (UTM) with a 1500 kN capacity, operating at a load rate of 0.3 kN/s, in compliance with EN 12390-6 [63]. During testing, the cylinder was positioned horizontally along its length at the center of the loading plate, as illustrated in Figure 7 (b). For each curing period and mix, three specimens were tested, and the average value was taken as the f_{st}. The splitting tensile strength was calculated using the equation outlined in Equation 2:

$$f_{st} = \frac{2 \times P_{max}}{\pi \times L \times D} \quad (2)$$

Flexural Strength Test

The flexural strength (f_s), was evaluated using beam specimens with dimensions of 100 × 100 × 350 mm, where the width (W) and height (H) were 100 mm, and the span length (L) was 300 mm. The beams were water-cured for 28 days prior to testing. The f_s was determined using a three-point bending test performed on a universal testing machine (UTM) with a 1500 kN capacity, applying a load rate of 0.1 kN/s in compliance with EN 12390-5 [64]. The setup followed ASTM C1018 [65] guidelines, employing a three-point loading configuration, as indicated in Figure 7 (c). For each mixing and curing period, the flexural strength was calculated as the average of three tested beams. The f_s was determined using the formula specified in Equation 3:

$$f_s = \frac{3 \times P_{max} \times L}{2 \times W \times H^2} \quad (3)$$

3.2. Water Porosity Test

The water porosity method, following the French AFPC-AFREM standard [38], was used to measure the total volume of water-accessible pores in concrete. The test involved concrete cubes from different mixes, including those without CFs and those with UT, BT, and NT CFs. Each cube, measuring 100 mm × 100 mm × 100 mm, was sectioned into eight smaller specimens (50 mm × 50 mm × 50 mm) using a water-cooled diamond saw (Figure 8) to maximize the surface area for water penetration. The specimens were then submerged in water for 56 days to achieve complete saturation. After immersion, the weight of the saturated dry surface (SSD) was recorded as W_a. Each sample was then placed in a wire basket, immersed in water and weighed using a beam balance to obtain W_c. After oven drying at 105°C for 7 days, the samples were cooled and reweighed to obtain W_b. Equation 4 was used to calculate the water absorption W_p, Equation 5 was used to calculate the total water porosity (P) according to the French AFPC-AFREM standard. Equations 6 and 7 were used to calculate open porosity (capillary pores) denotes P_a and closed porosity (air pores) denotes (P_u), respectively, according to GOST 12730.4-78.3 standard [66].

$$W_p(\%) = \frac{W_a - W_b}{W_b} \times 100 \quad (4)$$

$$P(\%) = W_p \times \frac{W_b}{W_a - W_c} \quad (5)$$

$$P_a(\%) = W_p \times \frac{\rho_b}{\rho_w} \quad (6)$$

$$P_u(\%) = \mathrm{P} - P_a \quad (7)$$

In the equations: ρ_b and ρ_w are the density of concrete and water, respectively.

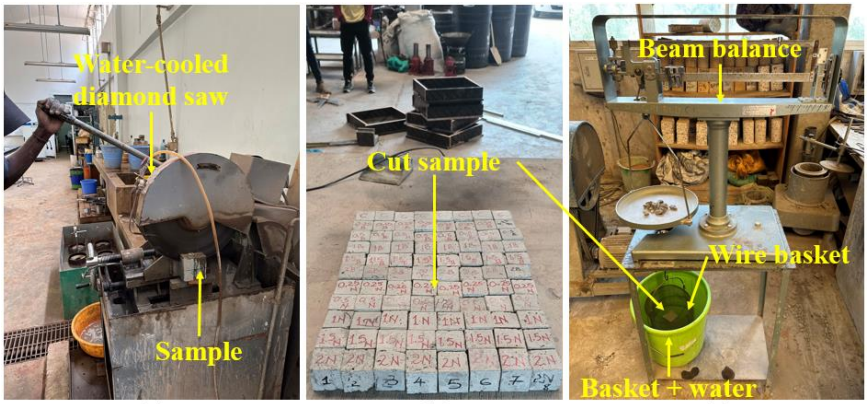

Figure 8. Preparing porosity samples: (a) cutting of concrete cube samples, (b) samples of cut concrete cube, and (c) measuring the weight of the saturated sample immersed in water

3.2. Resistance to Sulfuric Acid Test

The sulfuric acid resistance test was conducted following the guidelines of ASTM C267 (2006) [67]. Concrete cubes with dimensions of 100 mm per side were prepared and cured in water for 28 days. After curing, the cubes were air-dried for 7 days, weighed, and submerged in a 3% Sulfuric acid solution contained in plastic tanks for durations of 28 and 56 days, as illustrated in Figure 9. Upon removal from the acid solution, the samples were rinsed with water using a plastic brush, dried with an absorbent cloth, and weighed to calculate the percentage weight change. The cubes were subsequently tested for compressive strength to evaluate the percentage reduction. For each mix, three cubes were tested, and the average results were recorded.

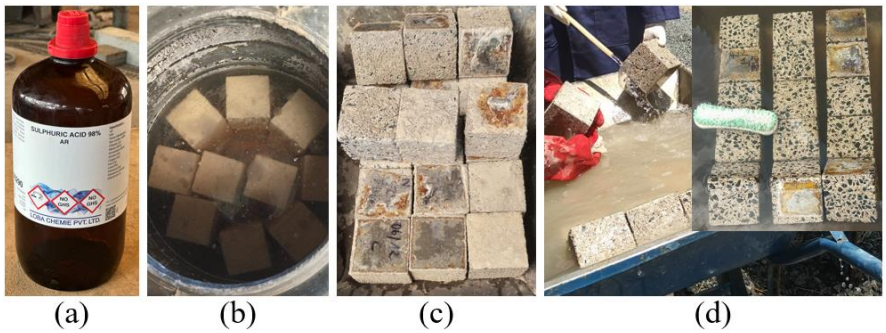

Figure 9. Sulfuric acid test: (a) sulfuric acid container (98% analytical reagent), (b) specimens immersed in sulfuric acid solution, (c) specimens removed from sulfuric acid solution, and (d) washing of specimens after removal from sulfuric acid solution.

4. Results and Discussion

4.1. Scanning Electron Microscopy (SEM) of Coconut Fibers

Figure 10 presents SEM images illustrating the morphology of UT, BT, and NT CFs. The UT fibers, shown in Figure 10(a), exhibit uneven surfaces with impurities such as hemicelluloses and waxes, which can hinder their adhesion to cement paste. This observation aligns with findings reported by Raju et al. [68]. In contrast, Figure 10(b) highlights the BT CFs, which show reduced impurities and increased surface roughness. These characteristics enhance their mechanical bonding with cement paste. Following the NT, the fibers exhibit cleaner and smoother surfaces, as seen in Figure 10(c), due to the removal of impurities. This treatment improves the fibers' contact area

and adhesion with the cement paste. Furthermore, the treated CFs demonstrate better friction resistance and lower water absorption, attributed to their compressed cellular structure, as supported by Mulinari et al. [69] and Zamboni et al. [70]. Reddy et al. [71] similarly noted that alkali-treated fibers exhibit a compressed cellular structure with fewer voids, which significantly reduces water absorption. This study further investigated the effects of NT CFs on the slump, strength and sulfuric acid resistance of HSC, as well as the influence of UT, BT, and NT CFs on the dry density and water porosity of HSC.

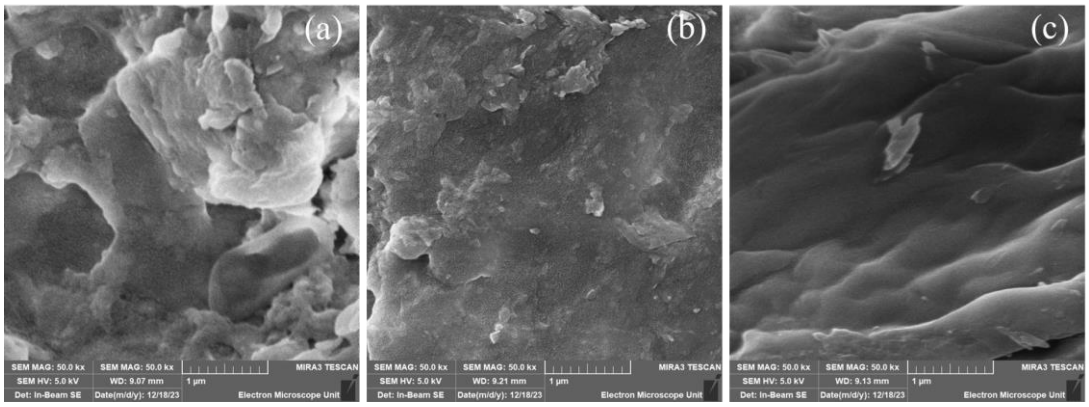

Figure 10. SEM analyses of the coconut fiber: (a) untreated, (b) boil-treated, and (c) NaOH-treated

4.2. Workability of Concrete

Concrete workability refers to the ease with which concrete can be placed, compacted, and finished without segregation or bleeding. It is a critical property influenced by factors such as the water-to-cement (W/C) ratio, fiber inclusion, aggregate type, and chemical admixtures. In this study, workability was evaluated using the slump test in accordance with ASTM C143/C143M standards [72]. Figure 11 illustrates the impact of NT CFs on the workability of HSC. The results indicate that increasing the NT CF content significantly decreases workability. This reduction is attributed to the higher surface area and irregular morphology of the fibers, which increase internal friction and require more cement paste to achieve sufficient lubrication, as noted by Ahmad et al. [73]. The control mix, incorporating 2% SP, achieved a slump of 176 mm. However, as the NT CF content increased, the slump values progressively decreased. Reductions in slump for 0.25, 0.5, 1, 1.5, and 2% CF content were recorded as 6.25, 12.01, 35.30, 63.70, and 92.60%, respectively. This decline in workability can lead to poor compaction, increased porosity in the hardened concrete, and subsequently, reduced strength, as supported by Ahmad et al. [74]. These findings align with previous studies, which have consistently reported a decrease in workability with the inclusion of coconut fibers. This reduction is primarily attributed to the fibers' ability to increase internal friction and disrupt the flow of the cement paste [73, 75, 76]. The practical implications of these results emphasize the need to balance fiber content and mix design to achieve both desired workability and mechanical performance. Adjustments, such as optimizing the use of SP or modifying the W/C ratio, can help mitigate the adverse effects of fibers on workability while leveraging their benefits in enhancing concrete's mechanical and fracture properties.

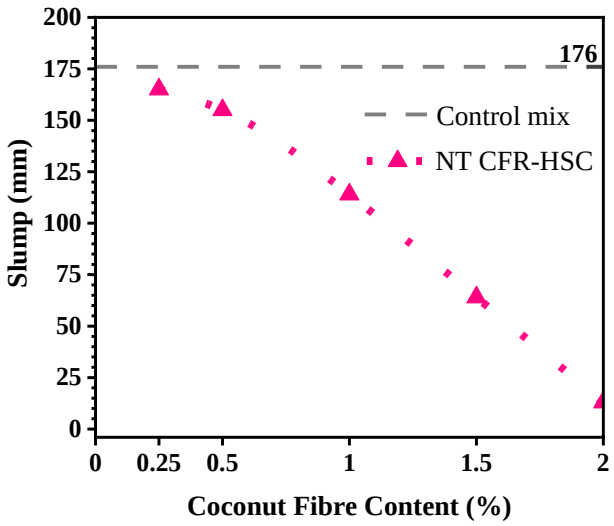

Figure 11. Workability of NaOH-treated coconut fiber reinforced high-strength concrete

4.3. Mechanical Strength

Compressive Strength

Figure 12 presents the failure modes of cube specimens under compression. In Figure 12(a), the control concrete cube, which contained no fibers, underwent brittle failure, characterized by a sudden and explosive detachment of concrete fragments at peak load. This behavior is attributed to the mix's high dry density and compressive strength, which result in rapid and catastrophic failure once the material reaches its load-bearing limit. In contrast, CFR-HSC cubes, shown in Figures 12(b) and 12(c), exhibited a more ductile failure mode. The presence of CFs helped maintain structural integrity, reducing fragmentation and preventing abrupt collapse. Specimens with lower fiber content (Figure 12b) developed multiple cracks at failure, while those with higher fiber content (Figure 12c) exhibited fewer but more controlled cracks, highlighting improved crack-bridging capability and greater post-peak load resistance.

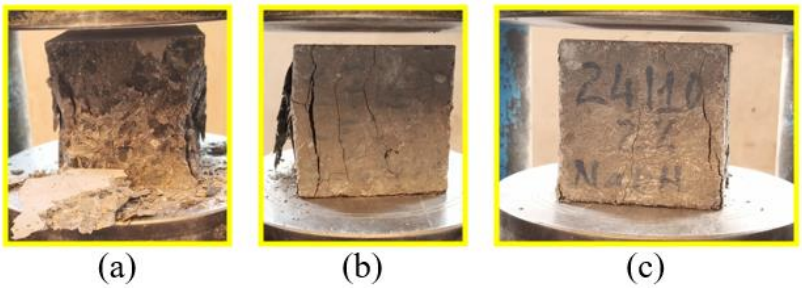

Figure 12. Failure modes of cube specimens: (a) control concrete cube, (b) concrete cube with low fiber content, and (c) concrete cube with high fiber content

Figure 13 illustrates the influence of NT CF on compressive strength of concrete. The control mix exhibited compressive strengths of 47.40, 53.54 and 67.56 MPa at 7, 14 and 28 days, respectively. The inclusion of 0.5% CF content resulted in a 2.31% increase in compressive strength after 7 days compared to the control mix. In contrast, other CF contents (0.25, 1, 1.5, and 2%) led to reductions of 11.26, 0.85, 1.91 and 8.54%, respectively. After 14 days of curing, all CFR-HSC samples exhibited compressive strength enhancements relative to the control mix. Specifically, compressive strength increased by 11.76, 13.03, 7.35, 5.66 and 4.72% for CF contents of 0.25, 0.5, 1, 1.5 and 2%, respectively. However, by the 28-day curing period, all reinforced concrete samples showed a decline in compressive strength compared to the control mix. The reductions recorded were 6.53, 5.72, 9.94, 13.29 and 14.10% for the same CF contents, respectively. These findings align with previous studies [46, 77]. The observed decrease in compressive strength at 28 days is primarily attributed to an increased water/cement ratio. NT CFs exhibit lower water absorption than UT or BT CFs. Consequently, incorporating 2% of SP by cement weight led to excessive workability, increasing the porosity of the concrete matrix and negatively impacting compressive strength. Furthermore, higher CF contents exacerbated porosity, as noted by Ren et al. [78]. An increased fiber contents create additional voids, reducing the concrete's density and subsequently weakening its compressive strength [79]. These voids serve as stress concentration points under loading conditions, accelerating crack propagation and compromising the structural integrity of the concrete. Despite the overall reduction in compressive strength at 28 days, concrete mixtures incorporating CF contents between 0.25 and 1% successfully achieved the target compressive strength of 60 MPa. This indicates that moderate fiber incorporation can enhance mechanical properties without significantly compromising strength. However, exceeding this range leads to excessive porosity, which diminishes the structural performance of the concrete.

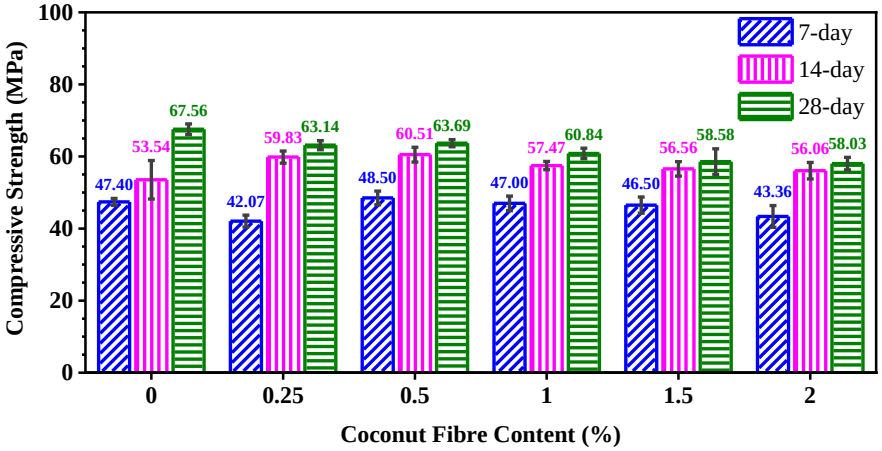

Figure 13. Effect of NaOH-treated coconut fiber on compressive strength of high-strength concrete

Splitting Tensile Strength

Figure 14 illustrates the failure modes of cylindrical specimens subjected to the split tensile strength test. In Figure 14(a), the control concrete cylinder, which contained no CFs, exhibited brittle failure, with some specimens splitting into two distinct pieces, while others developed wide cracks before failure. This behavior is typical of plain HSC, where the absence of fiber reinforcement results in a sudden and complete fracture upon reaching the tensile limit. In contrast, Figures 14(b) and 14(c) depict the failure modes of CFR-HSC cylinders, which developed smaller cracks, with some specimens showing only fine cracks. The presence of CFs enhanced crack resistance by bridging microcracks and more effectively distributing tensile stresses throughout the matrix. The specimen with lower fiber content (Figure 14(b)) exhibited wider cracks than the one with higher CF contents (Figure 14(c)). It was observed that increasing fiber content improves the crack-bridging effect, reduces crack width, and enhances the ductility of the concrete under tensile loading [80].

Figure 14. Failure modes of cylinder specimens: (a) control concrete cylinder, (b) concrete cylinder with low fiber content, and (c) concrete cylinder with high fiber content

Figure 15 presents the substantial effect of embedding NT CF on tensile strength of HSC. The control mix demonstrated tensile strengths of 2.76 MPa, 2.93 MPa, and 3.15 MPa after 7, 14 and 28 days of curing, respectively. The inclusion of NT CFs into HSC exhibited considerable enhancements in tensile strength across different fiber contents and curing durations [46]. After 7 days of curing, the incorporation of 0.25, 0.5, 1, 1.5 and 2% CF content resulted in tensile strength improvements of 17.31, 24.09, 26.92, 25.10 and 17.39%, respectively. Over a 14-day curing period, these enhancements were 14.03, 19.95, 22.96, 20.65 and 11.82%, respectively. At 28 days, the tensile strength gains reached 18.51, 32.23, 34.71, 15.71 and 8.41% for the corresponding fiber contents. These improvements are attributed to the NaOH treatment of the CFs, which significantly enhances their bonding with the concrete matrix. The treatment effectively removes impurities and non-cellulosic substances from the fiber surfaces, promoting a stronger adhesion between the fibers and the cementitious material. Additionally, the surface roughness of the CF is increased through this process, creating more opportunities for mechanical interlocking with the cement matrix and thereby reinforcing the bond strength. Furthermore, the NaOH treatment induces chemical modifications in the fiber structure that improve their dispersion within the concrete mix. Enhanced dispersion minimizes fiber clumping and ensures a more uniform distribution of reinforcement throughout the composite, optimizing stress transfer within the matrix. As a result, the concrete gains superior tensile strength due to the improved interaction between the CFs and the surrounding cementitious phase. The variations in tensile strength enhancement across different CF contents indicate that while moderate CF additions (0.5–1%) maximize the tensile performance, excessive CF content (2%) leads to a reduction in efficiency. This could be due to fiber agglomeration, which weakens the fiber-matrix interface and hinders stress transfer. Therefore, selecting an optimal fiber content is crucial to achieving maximum performance benefits from NT CFs in HSC applications.

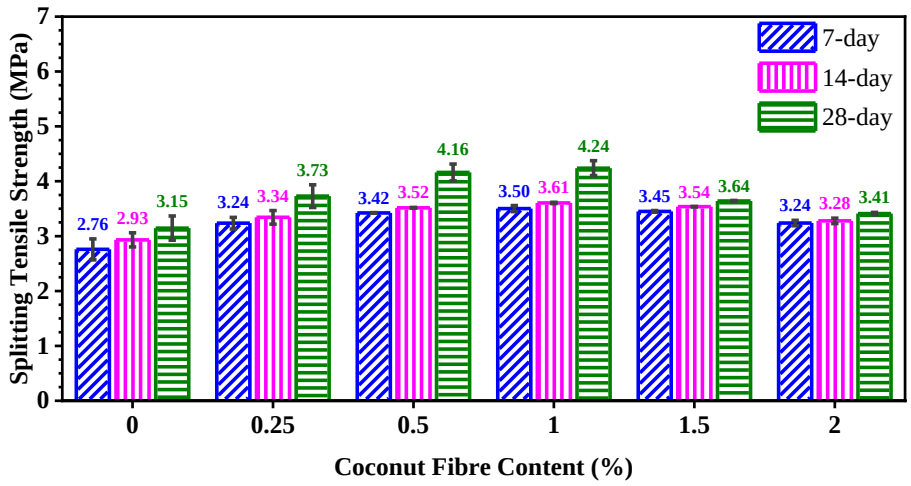

Figure 15. Effect of NaOH-treated coconut fiber on tensile strength of high-strength concrete

Flexural Strength

Figure 16 illustrates the failure modes of beam specimens under loading. The control concrete beam, which contained no CFs, exhibited sudden fragmentation at maximum load, indicating a brittle failure mode, as shown in Figure 16(a). This abrupt failure was due to the inability of the concrete matrix to redistribute stresses once cracking initiated. In contrast, the concrete beam reinforced with CFs, as shown in Figure 16(b), maintained its structural integrity even beyond the peak load. The presence of fibers effectively bridged cracks, delaying their propagation and preventing complete disintegration. This improved ductility is attributed to the fiber reinforcement, which enhanced post-cracking load-bearing capacity and energy absorption. Additionally, the control concrete beam developed a prominent crack at the midspan, whereas CFR-HSC beams exhibited smaller, more distributed cracks, further highlighting the beneficial effect of fiber reinforcement in mitigating sudden failure and improving fracture resistance.

(a) (b)

Figure 16. Failure modes of beam specimens: (a) control concrete beam and (b) fiber-reinforced concrete beam

Figure 17 illustrates the influence of NT CF on flexural strength of concrete after 28 days of curing. The control mix, exhibited a flexural strength of 6.01 MPa. The incorporation of CFs into the concrete mixture initially enhanced the flexural strength, reaching a peak at 1% CF content before exhibiting a slight decline at higher fiber contents [73]. The results indicate that as the CF contents increased from 0.25 to 1%, the flexural strength progressively improved, demonstrating the reinforcing potential of CFs in HSC. The highest flexural strength was achieved at 1% CF content, highlighting the optimal balance between fiber dispersion and matrix integrity. However, beyond this threshold, at CF contents of 1.5 and 2%, the flexural strength exhibited a declining trend. Notably, the concrete mix reinforced with NT CFs exhibited a flexural strength increase of 7.03% at 1% CF content and 3.21% at 1.5% CF content compared to the control mix. Conversely, at CF contents of 0.25, 0.5 and 2%, flexural strength declined by 6.73, 4.49 and 2.01%, respectively. These findings suggest that while moderate fiber incorporation enhances mechanical performance, excessive fiber content may lead to agglomeration and reduced stress transfer efficiency, thereby affecting flexural strength negatively. The improvement in flexural strength with NT CFs can be attributed to enhanced fiber-matrix interaction. The NaOH treatment process effectively removes impurities and surface oils from the fibers, increasing their roughness and improving their bonding with the concrete matrix.

This enhanced adhesion helps mitigate common issues such as fiber slippage and poor dispersion, which are typically responsible for reductions in flexural strength. Additionally, the increased contact surface area between treated fibers and the cementitious matrix contributes to better stress distribution and crack-bridging capability, further improving the flexural performance of the concrete. However, at higher fiber contents, the benefits of NaOH treatment are offset by fiber clustering and reduced workability, which may lead to localized weak zones in the concrete. This explains the observed reduction in flexural strength at 2% CF content. Thus, an optimal fiber content is necessary to maximize the reinforcing effect while minimizing adverse impacts on the concrete matrix. In summary, NT CFs significantly enhance the flexural strength of concrete when used in optimal proportions, with the best performance observed at 1% CF content. Beyond this level, reductions in flexural strength suggest that excessive fiber inclusion leads to dispersion challenges and matrix disruptions. The findings underscore the importance of proper fiber treatment and content optimization in developing the high performance of CFR-HSC.

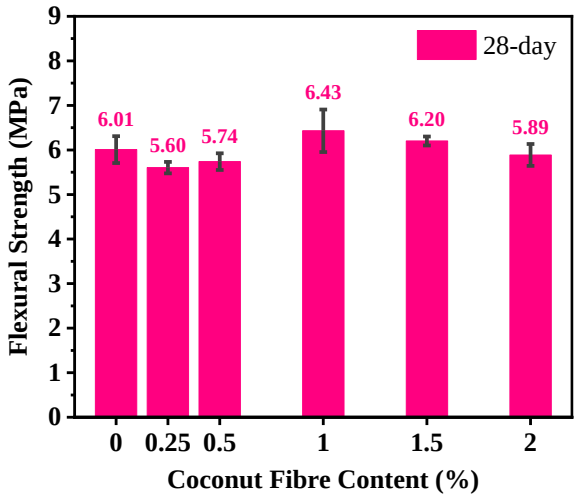

Figure 17. Effect of NaOH-treated coconut fiber on flexural strength of high-strength concrete

4.4. Dry Density of Hardened Concrete

The dry density of hardened concrete is defined as the ratio of its dry weight to the volume it occupies, expressed in kilograms per cubic meter (kg/m³). To determine this parameter, cubic samples with edge lengths of 100 mm were cured for 28 days and oven-dried at 105°C for 72 hours to remove moisture. The volume of each sample was measured using a 150 mm stainless steel digital caliper, and their weight was recorded with a precision balance. The average dry density for each concrete mix was calculated from three samples after curing.

Figure 18 illustrates the influence of CF content on the dry density of hardened concrete. The results indicate that the dry density decreases as the CF content increases, up to 2%, compared to the control mix, which had a dry density of 2373 kg/m³. For concrete with UT CFs, the reductions in dry density were 0.42, 1.18, 0.62, 2.18 and 3.19% for CF contents of 0.25, 0.5, 1, 1.5 and 2%, respectively. Concrete with BT CFs led to reductions of 0.22, 1.32, 1.46, 3.68 and 3.88% at the same fiber levels. Similarly, concrete with NT CFs had reductions of 1.83, 2.68, 3.34, 3.62 and 4.19%. These findings demonstrate that incorporating CFs reduce the dry density of concrete, with the effect becoming more significant as the fiber content increases [81]. This reduction in density is primarily attributed to the low density of the fibers and potential issues with improper compaction during the incorporation of fibers into fresh concrete. The reduction in density due to the addition of CFs results in lightweight concrete, which is beneficial for applications where weight reduction is critical, such as high-rise buildings or structures on weak soils. Lightweight concrete is also easier and more cost-effective to transport and handle, reducing construction costs and improving efficiency. However, the decrease in density is associated with increased void content and a less uniform microstructure, which negatively affects compressive strength and stiffness. Lower-density concrete has higher porosity, reducing its resistance to cracking, bending, and compressive deformation. It was observed that UT and BT CFs exhibited irregular trends in dry density reduction. This inconsistency may be due to the lack of significant improvements from fiber surface treatment and the presence of cork-like structures on the fiber surface, which influence density. Achieving uniform fiber distribution also remains a challenge. Uneven dispersion can lead to variability within the concrete, where areas with higher fiber concentrations may show lower density, while areas with fewer fibers may exhibit higher density.

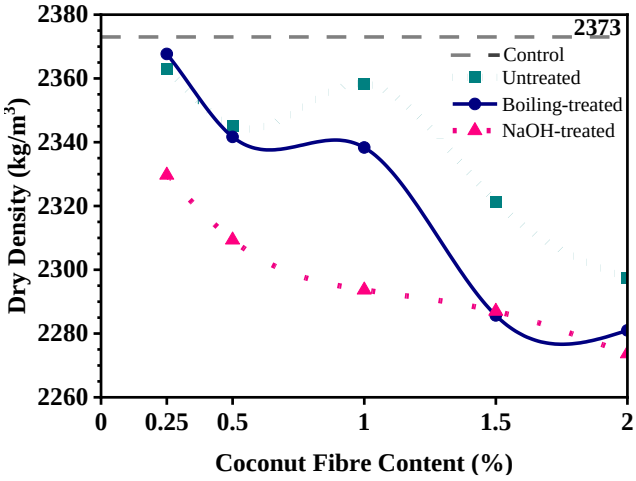

Figure 18. Effect of coconut fiber on the dry density of high-strength concrete

4.5. Durability Performances

Water Porosity

Figure 19 illustrates the effect of CFs on the porosity of concrete after 56 days of water curing. The control mix, without any added CFs, exhibited a total porosity of 11.22%, comprising 10.38% capillary porosity and 0.84% air porosity, as shown by the dashed line in Figure 19. The addition of CFs significantly increased the porosity of the concrete matrix, primarily due to their high-water absorption capacity. This property raises the water-to-cement ratio and slows the evaporation process, ultimately leading to higher porosity. Figure 19(a) reveals that the total porosity progressively increased with the addition of CFs. For concrete reinforced with UT CFs at 0.25 and 0.5% CF content, the total porosity decreased by 3.67 and 1.73%, respectively, compared to the control mix. However, higher CF contents of 1, 1.5 and 2% led to increases in total porosity by 5.90, 6.33 and 14.58%, respectively. A similar trend, albeit more pronounced, was observed with concrete reinforced with BT CFs. At 0.25 and 0.5% CF content, total porosity decreased by 4.20 and 2.97%, respectively, relative to the control mix, while at 1, 1.5, and 2% CF content, total porosity increased by 13.65, 16.29 and 21.52%, respectively. In contrast, NT CFs consistently increased total water porosity at all concrete with CF contents. Specifically, CF contents of 0.25, 0.5, 1, 1.5 and 2% resulted in increases of 19.08, 21.82, 26.45, 27.56 and 28.84%, respectively, compared to the control mix.

Figure 19(b) illustrates the impact of CFs on the capillary porosity of concrete, showing a trend that closely mirrors that of total porosity. In concrete reinforced with UT CFs, capillary porosity decreased by 0.42 and 0.94% at CF contents of 0.25 and 0.5%, respectively, compared to the control mix. However, higher CF contents of 1, 1.5, and 2% led to increases in capillary porosity by 6.21, 3.57 and 10.39%, respectively. A similar but more pronounced pattern was observed with BT CFs. At 0.25 and 0.5% CF content, capillary porosity decreased by 4.20 and 2.97%, respectively, while at 1, 1.5, and 2%, capillary porosity increased by 13.65, 16.29 and 21.52%. Conversely, NT CFs consistently increased capillary porosity at all concrete with CF contents, with increases of 16.82, 19.56, 22.41, 24.40 and 22.86% for 0.25, 0.5, 1, 1.5 and 2% CF content, respectively. This increase can be attributed to the higher water-to-cement ratio in mixes containing NT CFs, as these fibers absorb less water than UT and BT CFs, leaving more free water available in the mix [3]. Capillary porosity arises from several factors, including hydration, the paste-aggregate interface, and the formation of microcracks. Additionally, the high-water absorption capacity of CFs contributes to void formation at the fiber-matrix interface, which serves as water reservoirs. During mixing, a water film forms around the fibers due to their absorption and osmotic properties, causing them to expand [73]. As hydration progresses and water is consumed, this film dissipates, leaving voids at the interface. These voids adversely affect the compressive strength and durability [30, 31].

Figure 19(c) illustrates the air porosity values of concrete, determined by subtracting capillary porosity from total porosity. The results reveal that, the incorporation of CFs into concrete leads to an increase in air porosity as CF content rises. For concrete reinforced with UT CFs, air porosity initially decreased by 43.49 and 11.42% at CF contents of 0.25 and 0.5%, respectively, compared to the control mix. This reduction can be attributed to the improved packing of fibers at lower contents, which minimizes voids. However, at higher CF contents of 1, 1.5 and 2%, air porosity increased by 2.17, 40.24 and 66.12%, respectively, indicating that excessive CF contents introduce voids due to the disruption of the matrix's densification. A similar trend, though more pronounced, was observed in concrete reinforced with BT CFs. At 0.25, 0.5 and 1% CF content, air porosity decreased by 19.36, 6.82 and 0.89%, respectively, compared to the control mix.

However, at 1.5 and 2%, significant increases of 31.14 and 60.73% were recorded. The boiling treatment likely softens the fibers, making them more pliable and easier to distribute, but at higher contents, these fibers can create more voids. Conversely, NT CFs consistently increased air porosity across all concrete with CF contents. The air porosity rose by 46.79, 49.61, 76.08, 66.42 and 102.34% for fiber contents of 0.25, 0.5, 1, 1.5 and 2%, respectively. The NaOH treatment modifies the fiber surface, reducing water absorption and increasing stiffness, which can prevent proper compaction and lead to a greater number of voids in the matrix. These results suggest that while lower fiber contents can improve compaction and reduce air porosity, excessive fiber addition disrupts the matrix structure, creating more voids and significantly increasing air porosity, especially when fibers undergo chemical treatments like NaOH. This increase in air porosity can negatively impact the mechanical properties and durability of the concrete.

Resistance to Sulfuric Acid

Figure 20 presents the visual comparison of concrete samples with and without CFs after being cured in sulfuric acid and subjected to compressive strength tests. All samples exhibited surface damage, highlighting the vulnerability of concrete hydration products in the presence of sulfate ions. The exposure to sulfuric acid resulted in the formation of a white sludge layer on the surface, which can be attributed to the reaction of sulfate ions with calcium compounds in the concrete, as also observed in Figure 9(c). Additionally, Figure 20 and Figure 9(d) reveal that the acid exposure caused significant erosion and dissolution, leading to a roughened surface. This deterioration is primarily due to the dissolution of calcium silicate phases in the cement matrix when exposed to the sulfate-rich environment. The influence of sulfuric acid on HSC, both with and without CF reinforcements, was assessed by measuring the percentage loss in weight and strength following immersion in a 3% sulfuric acid solution. After compressive strength testing, the control mix

exhibited substantial detachment of concrete elements under peak load and displayed brittle failure, characterized by a sudden burst upon breaking. In contrast, the addition of CFs significantly improved the behavior of the concrete. CFR-HSC samples maintained the integrity of the concrete elements during failure and demonstrated a more ductile response. This ductile behavior became increasingly pronounced with higher fiber content, highlighting the reinforcing effect of CFs in mitigating the brittleness typically observed in HSC. Failure patterns were predominantly concentrated near specimen corners. Notably, CFR-HSC exhibited fewer and narrower cracks compared to the control mix. This improvement can be attributed to the fibers' ability to bridge microcracks and absorb energy, thereby enhancing the overall durability and resistance of the concrete under aggressive environmental conditions. These findings emphasize the beneficial role of CFs in enhancing the structural performance and durability of concrete exposed to sulfate-rich environments.

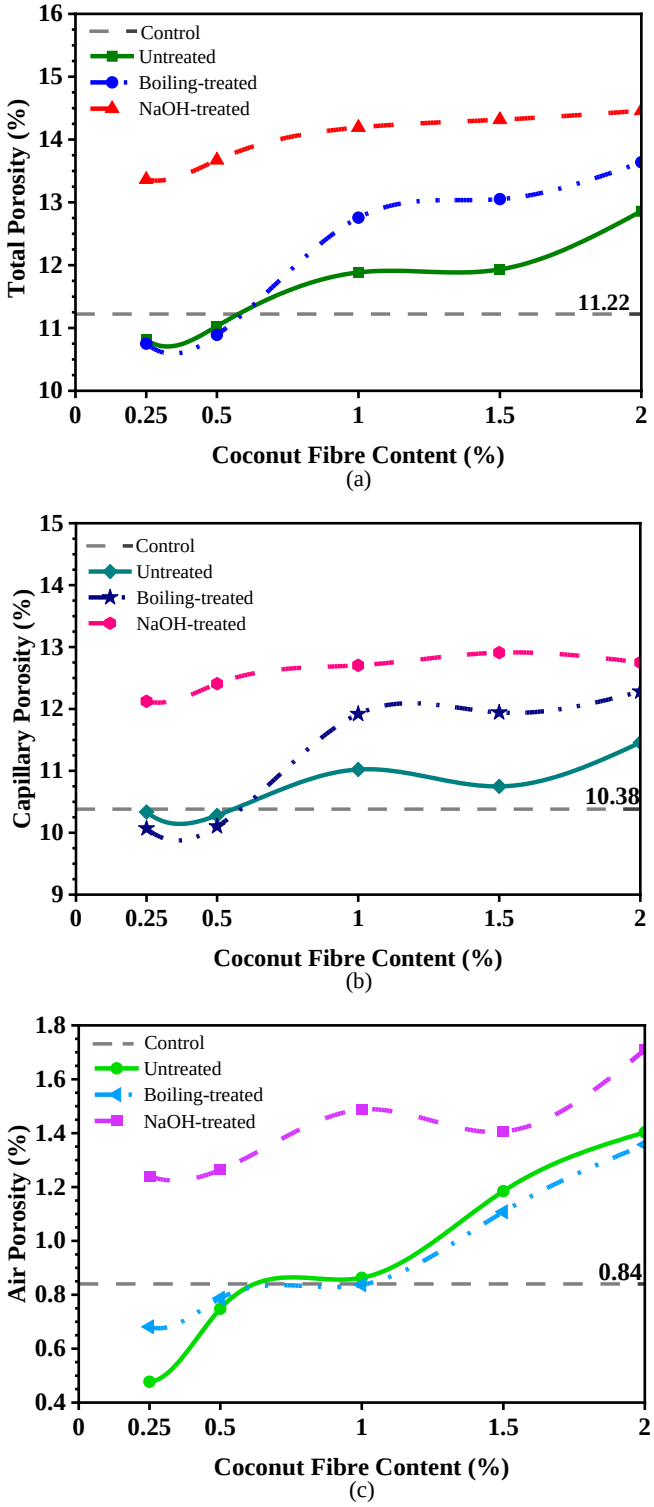

Figure 19. Water porosity of high-strength concrete reinforced with coconut fibers after 56 days for immersion in normal water: (a) total porosity, (b) capillary porosity, and (c) air porosity

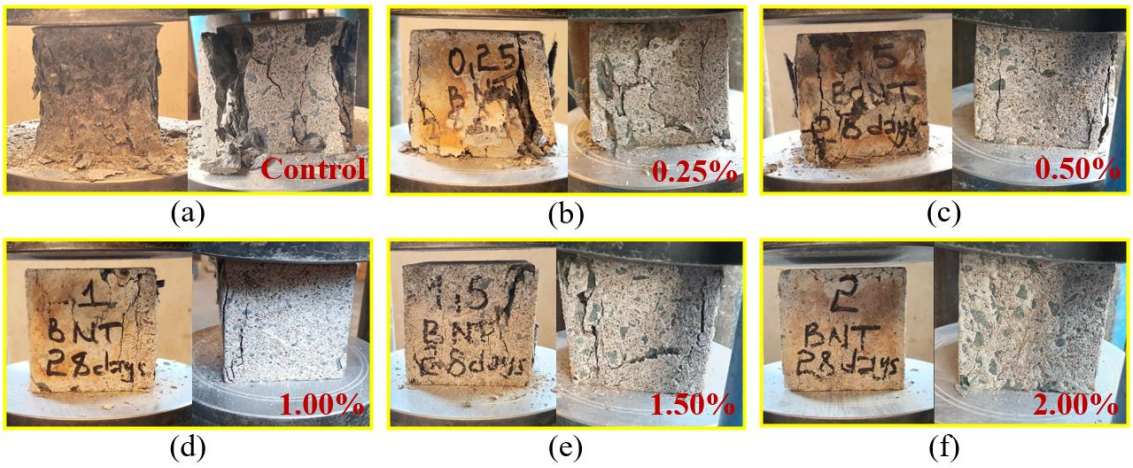

Figure 20. Visualization of samples with different fiber contents after curing in sulfuric acid and undergoing the compressive strength test

Figure 21 illustrates the percentage weight loss of HSC reinforced with NT CFs after 28 and 56 days of sulfuric acid exposure. All mixes experienced surface damage and weight loss due to the instability of concrete hydration products in the presence of sulfate ions, which compromise the matrix. The control mixes exhibited weight reductions of 3.17 and 3.68% after 28 and 56 days, respectively, highlighting its vulnerability to acid attack. The incorporation of CFs significantly reduced weight loss compared to the control mix, indicating improved resistance to acid-induced corrosion. After 28 days of exposure, weight losses for CFR-HSC were 1.14, 1.31, 1.43, 1.50 and 1.08% at CF contents of 0.25, 0.5, 1, 1.5 and 2%, respectively. A similar trend was observed after 56 days, with weight losses of 1.41, 1.56, 2.06, 2.51 and 1.39% for the same CF contents. These results suggest that fiber addition enhances the durability of concrete in sulfuric acid environments, with the greatest improvement observed at moderate to higher fiber contents. The reduction in weight loss can be attributed to the fibers' ability to limit crack formation and propagation, thereby reducing acid penetration into the matrix. By bridging microcracks, the fibers provide additional reinforcement and improve the matrix's integrity under chemical attack. However, the results also highlight the potential drawbacks of excessively high fiber contents. At 1.5 and 2% CF content, while initial acid resistance improved, prolonged exposure led to slightly higher weight losses compared to lower fiber contents, suggesting that excessive fibers may increase segregation and permeability, allowing greater acid ingress over time. Overall, the study demonstrates that incorporating NT CFs into concrete can enhance its acid resistance, particularly at optimized fiber contents. Properly balancing the fiber content is critical to maximize durability while avoiding adverse effects such as segregation and increased permeability.

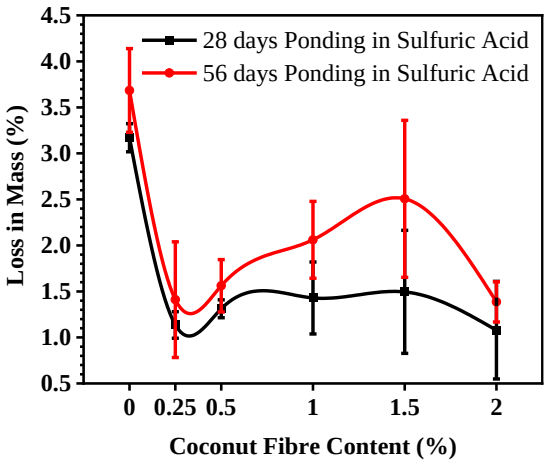

Figure 21. Percentage loss in Mass of high-strength concrete reinforced with NaOH-treated coconut-fibre under Sulfuric acid attack

Figure 22 presents the percentage loss in compressive strength of HSC reinforced with NT CFs after 28 and 56 days of sulfuric acid exposure. The control mix, without CFs, exhibited significant compressive strength reductions of 42.10% after 28 days and 53.08% after 56 days, highlighting its susceptibility to acid attack. The incorporation of NT CFs significantly mitigated strength loss, demonstrating the fibers' effectiveness in enhancing durability. After 28 days of acid exposure, compressive strength losses for CFR-HSC were 24.72, 19.91, 20.81, 24.78 and 26.94% at CF contents of 0.25, 0.5, 1, 1.5 and 2%, respectively. A similar trend was observed after 56 days, with compressive strength losses of 28.18, 25.62, 32.83, 35.66 and 36.33% for the same CF contents. These results indicate that fiber reinforcement significantly enhances acid resistance, particularly at moderate CF contents (0.5 and 1%), where the reduction in strength loss is most pronounced.

The strength degradation observed in sulfuric acid environments is primarily due to a chemical process known as sulfate attack. Sulfate ions react with the cementitious matrix, forming expansive compounds such as ettringite, which generate internal pressure, induce microcracks, and accelerate strength loss. Additionally, sulfuric acid exposure leads to surface erosion, cracking, and volume changes, further compromising the structural integrity of the concrete. The incorporation of NT CFs reduces these effects by limiting microcrack propagation and enhancing the concrete's resistance to acid penetration. The fibers act as physical barriers, shielding the cementitious materials from direct acid exposure while also reducing ettringite formation. Overall, the results demonstrate that adding NT CFs to HSC improves its durability in aggressive environments by reducing compressive strength loss and mitigating the effects of sulfate attack. However, excessively high CF contents (1.5 and 2%) show diminishing returns, as increased porosity may lead to a slight increase in strength loss over time. Optimizing fiber content is therefore crucial to maximizing acid resistance while maintaining structural integrity.

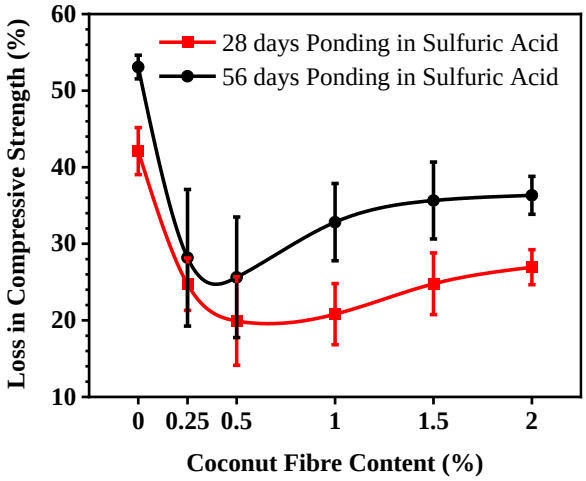

Figure 22. Percentage loss in compressive strength of high-strength concrete reinforced with NaOH-treated coconut-fibre under Sulfuric acid attack

5. Conclusion and Recommendations

This study investigated the effects of coconut fiber (CF) treatment on the strength properties, water porosity, and sulfuric acid resistance of high-strength concrete (HSC). Based on the findings, the following conclusions can be drawn:

- Scanning Electron Microscopy (SEM) analysis revealed that NaOH-treated (NT) CFs exhibited improved surface characteristics, enhancing their mechanical bonding with the cement matrix.
- The inclusion of NT CFs reduced workability and dry density, leading to increased porosity and, consequently, a decrease in compressive strength.
- The study demonstrated that NT CFs improved the tensile and flexural strengths of HSC, particularly at specific CF contents, due to enhanced bonding and stress transfer within the matrix. However, the inclusion of NT CFs did not significantly enhance the compressive strength of HSC. A reduction in compressive strength was observed at 28 days compared to the control mix (concrete without fibers). Despite this, coconut fiber-reinforced high-strength concrete (CFR-HSC) with CF contents between 0.25 and 1% successfully achieved the target compressive strength of 60 MPa.
- The incorporation of untreated (UT), boil-treated (BT), and NT CFs reduced the dry density of HSC compared to the control mix. The reduction was most significant with NT CFs, followed by BT CFs, and the least with UT CFs.
- The inclusion of CFs increased water porosity in all cases, with the highest increase observed in NT CFR-HSC, followed by BT CFR-HSC, and the lowest increase in UT CFR-HSC.
- The addition of NT CFs improved the durability of HSC in sulfuric acid environments. The greatest resistance was observed at moderate to higher CF contents, as the fibers helped limit crack formation and propagation, reducing acid penetration into the concrete matrix. By bridging microcracks, the fibers provided additional reinforcement and improved the integrity of the matrix under chemical attack.
- Further studies should investigate alternative treatment methods for CFs to evaluate their impact on the strength and long-term durability of HSC in various aggressive environments.
- The incorporation of pozzolanic materials in CFR-HSC is recommended to mitigate the porosity effect and enhance strength.
- Future research should carefully investigate the effects of high-range water-reducing admixtures (superplasticizers) on CFR-HSC to optimize workability, reduce porosity, and enhance strength and long-term durability.

6. Declarations

6.1. Author Contributions

Conceptualization, G.H.M.L.; methodology, G.H.M.L.; validation, J.N.M. and C.K.; investigation, G.H.M.L.; resources, G.H.M.L.; writing—original draft preparation, G.H.M.L.; writing—review and editing, G.H.M.L., J.N.M., C.K., and S.O.A.; supervision, J.N.M., C.K., and S.O.A.; funding acquisition, G.H.M.L. All authors have read and agreed to the published version of the manuscript.

6.2. Data Availability Statement

The data presented in this study are available in the article.

6.3. Funding

Gervany Hurlich Mboungou Londe reports financial support was provided by Pan African University Institute for Basic Sciences Technology and Innovation (PAUSTI), Nairobi, Kenya.

6.4. Acknowledgements

Pan African University (PAU) funds this research under a scholarship from the African Union (AU). The experimental tests were carried out at Jomo Kenyatta University of Agriculture and Technology (JKUAT), Nairobi, Kenya.

6.5. Conflicts of Interest

The authors declare no conflict of interest.

7. References

[1] Deng, Z., Liu, X., Yang, X., Liang, N., Yan, R., Chen, P., Miao, Q., & Xu, Y. (2021). A study of tensile and compressive properties of hybrid basalt-polypropylene fiber-reinforced concrete under uniaxial loads. Structural Concrete, 22(1), 396–409. doi:10.1002/suco.202000006.

[2] Liu, P., Zhou, X., Qian, Q., Berto, F., & Zhou, L. (2020). Dynamic splitting tensile properties of concrete and cement mortar. Fatigue and Fracture of Engineering Materials and Structures, 43(4), 757–770. doi:10.1111/ffe.13162.

[3] Mboungou Londe, G. H., Mwero, J. N., Kanali, C., & Abuodha, S. O. (2024). Investigating the Influence of Raw and Treated Coconut Fibre Obtained from Agricultural Residue on the Strength and Durability Characteristics of High-Strength Concrete. Advances in Civil Engineering, 2024. doi:10.1155/2024/8275876.

[4] Anurangi, J., Herath, M., Galhena, D. T. L., & Epaarachchi, J. (2023). The use of fibre reinforced polymer composites for construction of structural supercapacitors: a review. Advanced Composite Materials, 32(6), 942–986. doi:10.1080/09243046.2023.2180792.

[5] Mahboob, A., Hassanshahi, O., Safi, M., & Majid, T. A. (2024). Experimental investigation of eco-friendly fiber-reinforced concrete using recycled and natural fibers, integrated with recycled aggregates. Advanced Composite Materials, 33, 1101–30. doi:10.1080/09243046.2024.2322799.

[6] Rocha, D. L., Júnior, L. U. D. T., Marvila, M. T., Pereira, E. C., Souza, D., & de Azevedo, A. R. G. (2022). A Review of the Use of Natural Fibers in Cement Composites: Concepts, Applications and Brazilian History. Polymers, 14(10), 2043. doi:10.3390/polym14102043.

[7] Teng, S., Afroughsabet, V., & Ostertag, C. P. (2018). Flexural behavior and durability properties of high performance hybrid-fiber-reinforced concrete. Construction and Building Materials, 182, 504–515. doi:10.1016/j.conbuildmat.2018.06.158.

[8] Senthilkumar, K., Saba, N., Rajini, N., Chandrasekar, M., Jawaid, M., Siengchin, S., & Alotman, O. Y. (2018). Mechanical properties evaluation of sisal fibre reinforced polymer composites: A review. Construction and Building Materials, 174, 713–729. doi:10.1016/j.conbuildmat.2018.04.143.

[9] Aarthipriya, V., & Umarani, C. (2025). An ecofriendly approach to explore the physical and mechanical properties of cement mortar reinforced with Abutilon indicum fibres. Materials Research Express, 12(1), 015102. doi:10.1088/2053-1591/ada7ca.

[10] Chavan, S., & Rao, P. (2016). Utilization of Waste PET bottle fibers in concrete as an Innovation in Building Materials. International Journal of Engineering Research, 5(1), 304-307.

[11] Alomayri, T., & Ali, B. (2023). Effect of plant fiber type and content on the strength and durability performance of high-strength concrete. Construction and Building Materials, 394(132166). doi:10.1016/j.conbuildmat.2023.132166.

[12] Liew, K. M., & Akbar, A. (2020). The recent progress of recycled steel fiber reinforced concrete. Construction and Building Materials, 232(117232). doi:10.1016/j.conbuildmat.2019.117232.

[13] Ahmad, J., & Zhou, Z. (2022). Mechanical Properties of Natural as well as Synthetic Fiber Reinforced Concrete: A Review. Construction and Building Materials, 333, 127353. doi:10.1016/j.conbuildmat.2022.127353.

[14] Jamshaid, H., Mishra, R. K., Raza, A., Hussain, U., Rahman, M. L., Nazari, S., Chandan, V., Muller, M., & Choteborsky, R. (2022). Natural Cellulosic Fiber Reinforced Concrete: Influence of Fiber Type and Loading Percentage on Mechanical and Water Absorption Performance. Materials, 15(3), 874. doi:10.3390/ma15030874.

[15] Martinelli, F. R. B., Ribeiro, F. R. C., Marvila, M. T., Monteiro, S. N., Filho, F. da C. G., & Azevedo, A. R. G. de. (2023). A Review of the Use of Coconut Fiber in Cement Composites. Polymers, 15(5), 1309. doi:10.3390/polym15051309.

[16] Zakaria, M., Ahmed, M., Hoque, M. M., & Islam, S. (2017). Scope of using jute fiber for the reinforcement of concrete material. Textiles and Clothing Sustainability, 2(1), 1–10. doi:10.1186/s40689-016-0022-5.

[17] . T. S. V. K. (2016). A Comparative Study of Jute Fiber Reinforced Concrete with Plain Cement Concrete. International Journal of Research in Engineering and Technology, 05(09), 111–116. doi:10.15623/ijret.2016.0509017.

[18] Fokam, C. B., Toumi, E., Kenmeugne, B., Meva'A, L., & Mansouri, K. (2020). Cement mortar reinforced with palm nuts naturals fibers: Study of the mechanical properties. Journal of Composites and Advanced Materials, 30(1), 9–13. doi:10.18280/rcma.300102.

[19] Soltanzadeh, F., Barros, J. A. O., & Santos, R. F. C. (2015). High performance fiber reinforced concrete for the shear reinforcement: Experimental and numerical research. Construction and Building Materials, 77, 94–109. doi:10.1016/j.conbuildmat.2014.12.003.

[20] Nambiar, R. A., & Haridharan, M. K. (2019). Mechanical and durability study of high performance concrete with addition of natural fiber (jute). Materials Today: Proceedings, 46, 4941–4947. doi:10.1016/j.matpr.2020.10.339.

[21] Alsaif, A., Koutas, L., Bernal, S. A., Guadagnini, M., & Pilakoutas, K. (2018). Mechanical performance of steel fibre reinforced rubberised concrete for flexible concrete pavements. Construction and Building Materials, 172, 533–543. doi:10.1016/j.conbuildmat.2018.04.010.

[22] Wuest, J., Denarié, E., Brühwiler, E., Tamarit, L., Kocher, M., & Gallucci, E. (2009). Tomography analysis of fiber distribution and orientation in ultra-high-performance fiber reinforced composites with high-fiber dosages. Experimental Techniques, 33(5), 50–55. doi:10.1111/j.1747-1567.2008.00420.x.

[23] Stähli, P., Custer, R., & Van Mier, J. G. M. (2008). On flow properties, fibre distribution, fibre orientation and flexural behaviour of FRC. Materials and Structures, 41(1), 189–196. doi:10.1617/s11527-007-9229-x.

[24] Tejchman, J., & Kozicki, J. (2010). Experimental and theoretical investigations of steel-fibrous concrete. Springer, Berlin, Germany. doi:10.1007/978-3-642-14603-9.

[25] Eik, M., Lõhmus, K., Tigasson, M., Listak, M., Puttonen, J., & Herrmann, H. (2013). DC-conductivity testing combined with photometry for measuring fibre orientations in SFRC. Journal of Materials Science, 48(10), 3745–3759. doi:10.1007/s10853-013-7174-3.

[26] Revilla-Cuesta, V., Faleschini, F., Pellegrino, C., Skaf, M., & Ortega-López, V. (2024). Water transport and porosity trends of concrete containing integral additions of raw-crushed wind-turbine blade. Developments in the Built Environment, 17, 100374. doi:10.1016/j.dibe.2024.100374.

[27] Santamaría, A., Orbe, A., San José, J. T., & González, J. J. (2018). A study on the durability of structural concrete incorporating electric steelmaking slags. Construction and Building Materials, 161, 94–111. doi:10.1016/j.conbuildmat.2017.11.121.

[28] Cantero, B., Sáez del Bosque, I. F., Sánchez de Rojas, M. I., Matías, A., & Medina, C. (2022). Durability of concretes bearing construction and demolition waste as cement and coarse aggregate substitutes. Cement and Concrete Composites, 134, 104722. doi:10.1016/j.cemconcomp.2022.104722.

[29] Faleschini, F., Alejandro Fernández-Ruíz, M., Zanini, M. A., Brunelli, K., Pellegrino, C., & Hernández-Montes, E. (2015). High performance concrete with electric arc furnace slag as aggregate: Mechanical and durability properties. Construction and Building Materials, 101, 113–121. doi:10.1016/j.conbuildmat.2015.10.022.

[30] Vu, V. H., Tran, B. V., Hoang, V. H., & Nguyen, T. H. G. (2022). The Effect of Porosity on the Elastic Modulus and Strength of Pervious Concrete. Lecture Notes in Mechanical Engineering, 823–829. doi:10.1007/978-981-16-3239-6_63.

[31] Revilla-Cuesta, V., Skaf, M., Santamaría, A., Romera, J. M., & Ortega-López, V. (2022). Elastic stiffness estimation of aggregate–ITZ system of concrete through matrix porosity and volumetric considerations: explanation and exemplification. Archives of Civil and Mechanical Engineering, 22(2), 59. doi:10.1007/s43452-022-00382-z.

[32] Abhilash, P. P., Nayak, D. K., Sangoju, B., Kumar, R., & Kumar, V. (2021). Effect of nano-silica in concrete; a review. Construction and Building Materials, 278, 122347. doi:10.1016/j.conbuildmat.2021.122347.

[33] Moore, A. J., Bakera, A. T., & Alexander, M. G. (2021). A critical review of the Water Sorptivity Index (WSI) parameter for potential durability assessment: Can WSI be considered in isolation of porosity? Journal of the South African Institution of Civil Engineering, 63(2), 27–34. doi:10.17159/2309-8775/2021/v63n2a4.

[34] Rahman, S., Grasley, Z., Masad, E., Zollinger, D., Iyengar, S., & Kogbara, R. (2016). Simulation of Mass, Linear Momentum, and Energy Transport in Concrete with Varying Moisture Content during Cooling to Cryogenic Temperatures. Transport in Porous Media, 112(1), 139–166. doi:10.1007/s11242-016-0636-8.

[35] Sivamani, J., & Renganathan, N. T. (2022). Effect of fine recycled aggregate on the strength and durability properties of concrete modified through two-stage mixing approach. Environmental Science and Pollution Research, 29(57), 85869–85882. doi:10.1007/s11356-021-14420-5.

[36] Cantero, B., Sáez del Bosque, I. F., Matías, A., Sánchez de Rojas, M. I., & Medina, C. (2020). Water transport mechanisms in concretes bearing mixed recycled aggregates. Cement and Concrete Composites, 107, 103486. doi:10.1016/j.cemconcomp.2019.103486.

[37] Villagrán Zaccardi, Y. A., Alderete, N. M., & De Belie, N. (2017). Improved model for capillary absorption in cementitious materials: Progress over the fourth root of time. Cement and Concrete Research, 100, 153–165. doi:10.1016/j.cemconres.2017.07.003.

[38] Joorabchian, S. M. (2010). Durability of concrete exposed to sulfuric acid attack. Doctoral Dissertation, Toronto Metropolitan University, Toronto, Canada.

[39] Vélez, E., Rodríguez, R., Yanchapanta Gómez, N. B., Mora, E. D., Hernández, L., Albuja-Sánchez, J., & Calvo, M. I. (2022). Coconut-Fiber Composite Concrete: Assessment of Mechanical Performance and Environmental Benefits. Fibers, 10(11), 96. doi:10.3390/fib10110096.

[40] Lv, C., & Liu, J. (2023). Alkaline Degradation of Plant Fiber Reinforcements in Geopolymer: A Review. Molecules, 28(4), 1868. doi:10.3390/molecules28041868.

[41] Rocha Ferreira, S., Ukrainczyk, N., Defáveri do Carmo e Silva, K., Eduardo Silva, L., & Koenders, E. (2021). Effect of microcrystalline cellulose on geopolymer and Portland cement pastes mechanical performance. Construction and Building Materials, 288, 123053. doi:10.1016/j.conbuildmat.2021.123053.

[42] da Costa Correia, V., Ardanuy, M., Claramunt, J., & Savastano, H. (2019). Assessment of chemical and mechanical behavior of bamboo pulp and Nano fibrillated cellulose exposed to alkaline environments. Cellulose, 26(17), 9269–9285. doi:10.1007/s10570-019-02703-7.

[43] Wei, J., & Meyer, C. (2015). Degradation mechanisms of natural fiber in the matrix of cement composites. Cement and Concrete Research, 73, 1–16. doi:10.1016/j.cemconres.2015.02.019.

[44] Labib, W. A. (2022). Plant-based fibres in cement composites: A conceptual framework. Journal of Engineered Fibers and Fabrics, 17. doi:10.1177/15589250221078922.

[45] Hamada, H. M., Shi, J., Al Jawahery, M. S., Majdi, A., Yousif, S. T., & Kaplan, G. (2023). Application of natural fibres in cement concrete: A critical review. Materials Today Communications, 35, 105833. doi:10.1016/j.mtcomm.2023.105833.

[46] Antwi-Afari, B. A., Mutuku, R., Kabubo, C., Mwero, J., & Mengo, W. K. (2024). Influence of fiber treatment methods on the mechanical properties of high strength concrete reinforced with sisal fibers. Heliyon, 10(8), e29760. doi:10.1016/j.heliyon.2024.e29760.

[47] Ali, A., Shaker, K., Nawab, Y., Jabbar, M., Hussain, T., Militky, J., & Baheti, V. (2018). Hydrophobic treatment of natural fibers and their composites—A review. Journal of Industrial Textiles, 47(8), 2153–2183. doi:10.1177/1528083716654468.

[48] Yavuz Bayraktar, O., Kaplan, G., Shi, J., Benli, A., Bodur, B., & Turkoglu, M. (2023). The effect of steel fiber aspect-ratio and content on the fresh, flexural, and mechanical performance of concrete made with recycled fine aggregate. Construction and Building Materials, 368, 130497. doi:10.1016/j.conbuildmat.2023.130497.

[49] Tran, N. P., Gunasekara, C., Law, D. W., Houshyar, S., & Setunge, S. (2022). Microstructural characterisation of cementitious composite incorporating polymeric fibre: A comprehensive review. Construction and Building Materials, 335, 127497. doi:10.1016/j.conbuildmat.2022.127497.

[50] Ortega-López, V., Revilla-Cuesta, V., Santamaría, A., Orbe, A., & Skaf, M. (2022). Microstructure and Dimensional Stability of Slag-Based High-Workability Concrete with Steelmaking Slag Aggregate and Fibers. Journal of Materials in Civil Engineering, 34(9), 04022224. doi:10.1061/(asce)mt.1943-5533.0004372.

[51] Camille, C., Kahagala Hewage, D., Mirza, O., Mashiri, F., Kirkland, B., & Clarke, T. (2021). Performance behaviour of macro-synthetic fibre reinforced concrete subjected to static and dynamic loadings for sleeper applications. Construction and Building Materials, 270, 121469. doi:10.1016/j.conbuildmat.2020.121469.

[52] Xie, J., Kou, S. cong, Ma, H., Long, W. J., Wang, Y., & Ye, T. H. (2021). Advances on properties of fiber reinforced recycled aggregate concrete: Experiments and models. Construction and Building Materials, 277, 122345. doi:10.1016/j.conbuildmat.2021.122345.

[53] Muthukumarana, T. V., Arachchi, M. A. V. H. M., Somarathna, H. M. C. C., & Raman, S. N. (2023). A review on the variation of mechanical properties of carbon fibre-reinforced concrete. Construction and Building Materials, 366, 130173. doi:10.1016/j.conbuildmat.2022.130173.

[54] EN 197-1. (2000). Cement - Part 1: Composition, Specifications and Conformity Criteria for Common Cements Ciment. European Standard, 1–29.

[55] ASTM C33. (2013). Standard specification for concrete aggregates. American Society for Testing and Materials (ASTM), Pennsylvania, United States.

[56] C136/C136M–14. (2014). Standard test method for sieve analysis of fine and coarse aggregates. American Society for Testing and Materials (ASTM), Pennsylvania, United States.

[57] BS812-2:1995. (2004). Testing aggregates Part 2. Methods of determination of density Corrected. British Standard, London, United Kingdom.

[58] ASTM C127. (2004). Standard Test Method for Density, Relative Density (Specific Gravity), and Absorption of Coarse Aggregate. American Society for Testing and Materials (ASTM), Pennsylvania, United States.

[59] BS 812-112:1990. (1990). Testing aggregates- part 112: Methods for determination of aggregate impact value (AIV). British Standard, London, United Kingdom.

[60] BS 812-110: 1990. (1990). Testing aggregates - part 110: Methods for determination of aggregate crushing value (ACV). British Standard, London, United Kingdom.

[61] ACI 211.4R. (2008). Guide for Selecting Proportions for High-strength Concrete Using Portland Cement and Other Cementitious Materials. ACI Committee 211, 1–25.

[62] BS EN 12390-3. (2009). Testing hardened concrete - Part 3: Compressive strength of test specimens. BSI Standards, 38(10), 18.

[63] BS EN 12390-6. (2009). Testing hardened concrete - Part 6: Tensile splitting strength of test specimens. BSI Standards, 1–14.

[64] BS EN 12390-5. (2009). Testing hardened concrete - Part 5: Flexural strength of test specimens. BSI Standards, 1–22.

[65] ASTM C1018. (1998). Standard Test Method for Flexural Toughness and First-Crack Strength of Fiber-Reinforced Concrete (Using Beam with Third-Point Loading). American Society for Testing and Materials (ASTM), Pennsylvania, United States.

[66] Daukšys, M., Ivanauskas, E., Juočiunas, S., Pupeikis, D., & Šeduikyte, L. (2012). The assessment of prediction methodology of concrete freezing and thawing resistance. Medziagotyra, 18(4), 403–409. doi:10.5755/j01.ms.18.4.3105.

[67] ASTM C 267. (2001). Standard Test Methods for Chemical Resistance of Mortars, Grouts, and Monolithic Surfacings and Polymer Concretes. American Society for Testing and Materials (ASTM), Pennsylvania, United States.

[68] Raju, J. S. N., Depoures, M. V., & Kumaran, P. (2021). Comprehensive characterization of raw and alkali (NaOH) treated natural fibers from Symphirema involucratum stem. International Journal of Biological Macromolecules, 186, 886–896. doi:10.1016/j.ijbiomac.2021.07.061.

[69] Mulinari, D. R., Baptista, C. A. R. P., Souza, J. V. C., & Voorwald, H. J. C. (2011). Mechanical properties of coconut fibers reinforced polyester composites. Procedia Engineering, 10, 2074–2079. doi:10.1016/j.proeng.2011.04.343.

[70] Zamboni Schiavon, J., & de Oliveira Andrade, J. J. (2023). Comparison between alternative chemical treatments on coir fibers for application in cementitious materials. Journal of Materials Research and Technology, 25, 4634–4649. doi:10.1016/j.jmrt.2023.06.210.

[71] Reddy, K. O., Reddy, K. R. N., Zhang, J., Zhang, J., & Varada Rajulu, A. (2013). Effect of Alkali Treatment on the Properties of Century Fiber. Journal of Natural Fibers, 10(3), 282–296. doi:10.1080/15440478.2013.800812.

[72] ASTM C143/C143M. (2015). Standard Test Method for Slump of Hydraulic-Cement Concrete. American Society for Testing and Materials (ASTM), Pennsylvania, United States.

[73] Ahmad, J., Majdi, A., Al-Fakih, A., Deifalla, A. F., Althoey, F., El Ouni, M. H., & El-Shorbagy, M. A. (2022). Mechanical and Durability Performance of Coconut Fiber Reinforced Concrete: A State-of-the-Art Review. Materials, 15(10), 3601. doi:10.3390/ma15103601.

[74] Ahmad, W., Farooq, S. H., Usman, M., Khan, M., Ahmad, A., Aslam, F., Alyousef, R., Abduljabbar, H. Al, & Sufian, M. (2020). Effect of coconut fiber length and content on properties of high strength concrete. Materials, 13(5), 1075. doi:10.3390/ma13051075.

[75] Ahmad, J., Zaid, O., Siddique, M. S., Aslam, F., Alabduljabbar, H., & Khedher, K. M. (2021). Mechanical and durability characteristics of sustainable coconut fibers reinforced concrete with incorporation of marble powder. Materials Research Express, 8(7), 075505. doi:10.1088/2053-1591/ac10d3.

[76] Sivakumaresa Chockalingam, L. N., & Rymond, N. M. (2022). Strength and Durability Characteristics of Coir, Kenaf and Polypropylene Fibers Reinforced High Performance Concrete. Journal of Natural Fibers, 19(13), 6692–6700. doi:10.1080/15440478.2021.1929656.

[77] Okeola, A. A., Abuodha, S. O., & Mwero, J. (2018). Experimental investigation of the physical and mechanical properties of sisal fiber-reinforced concrete. Fibers, 6(3), 53. doi:10.3390/fib6030053.

[78] Ren, G., Yao, B., Huang, H., & Gao, X. (2021). Influence of sisal fibers on the mechanical performance of ultra-high performance concretes. Construction and Building Materials, 286, 122958. doi:10.1016/j.conbuildmat.2021.122958.

[79] Bentchikou, M., Guidoum, A., Scrivener, K., Silhadi, K., & Hanini, S. (2012). Effect of recycled cellulose fibres on the properties of lightweight cement composite matrix. Construction and Building Materials, 34, 451–456. doi:10.1016/j.conbuildmat.2012.02.097.

[80] Bui, H., Sebaibi, N., Boutouil, M., & Levacher, D. (2020). Determination and review of physical and mechanical properties of raw and treated coconut fibers for their recycling in construction materials. Fibers, 8(6), 37. doi:10.3390/FIB8060037.

[81] Naamandadin, N. A., Rosdi, M. S., Mustafa, W. A., Shahrol Aman, M. N. S., & Saidi, S. A. (2020). Mechanical behaviour on concrete of coconut coir fiber as additive. IOP Conference Series: Materials Science and Engineering, 932(1), 012098. doi:10.1088/1757-899X/932/1/012098.